Mol Neurobiol (2018) 55:1054–1067
DOI 10.1007/s12035-016-0376-3

Role of Dopamine D2/D3 Receptors in Development, Plasticity, and Neuroprotection in Human iPSC-Derived Midbrain Dopaminergic Neurons

Federica Bono[1] · Paola Savoia[1] · Adele Guglielmi[1] · Massimo Gennarelli[2,3] · Giovanna Piovani[2] · Sandra Sigala[1] · Damiana Leo[4] · Stefano Espinoza[4] · Raul R. Gainetdinov[4,5,6] · Paola Devoto[7] · PierFranco Spano[1,8] · Cristina Missale[1,8] · Chiara Fiorentini[1]

Received: 4 July 2016 / Accepted: 28 December 2016 / Published online: 14 January 2017

Abstract The role of dopamine D2 and D3 receptors (D2R/D3R), located on midbrain dopaminergic (DA) neurons, in the regulation of DA synthesis and release and in DA neuron homeostasis has been extensively investigated in rodent animal models. By contrast, the properties of D2R/D3R in human DA neurons have not been elucidated yet. On this line, the use of human-induced pluripotent stem cells (hiPSCs) for producing any types of cells has offered the innovative opportunity for investigating the human neuronal phenotypes at the molecular levels. In the present study, hiPSCs generated from human dermal fibroblasts were used to produce midbrain DA (mDA) neurons, expressing the proper set of genes and proteins typical of authentic, terminally differentiated DA neurons. In this model, the expression and the functional properties of the human D2R/D3R were investigated with a combination of biochemical and functional techniques. We observed that in hiPSC-derived mDA neurons, the activation of D2R/D3R promotes the proliferation of neuronal progenitor cells. In addition, we found that D2R/D3R activation inhibits nicotine-stimulated DA release and exerts neurotrophic effects on mDA neurons that likely occur via the activation of PI3K-dependent mechanisms. Furthermore, D2R/D3R stimulation counteracts both the aggregation of alpha-synuclein induced by glucose deprivation and the associated neuronal damage affecting both the soma and the dendrites of mDA neurons. Taken together, these data point to the D2R/D3R-related signaling events as a biochemical pathway crucial for supporting both neuronal development and survival and protection of human DA neurons.

Keywords hiPSC · Dopamine D2/D3 receptor · Neuroplasticity · Nicotine · Neurodegeneration · Development

Electronic supplementary material The online version of this article (doi:10.1007/s12035-016-0376-3) contains supplementary material, which is available to authorized users.

✉ Federica Bono
federica.bono@unibs.it

[1] Division of Pharmacology, Department of Molecular and Translational Medicine, University of Brescia, 25123 Brescia, Italy

[2] Section of Biology and Genetic, Department of Molecular and Translational Medicine, University of Brescia, 25123 Brescia, Italy

[3] Section of Genetics, IRCCS "Centro S. Giovanni di Dio" Fatebenefratelli, Brescia, Italy

[4] Department of Neuroscience and Brain Technologies, Italian Institute of Technology (IIT), 16163 Genova, Italy

[5] Institute of Translational Biomedicine, St. Petersburg State University, St. Petersburg 199034, Russia

[6] Skolkovo Institute of Science and Technology (Skoltech) Skolkovo, Moscow Region 143025, Russia

[7] Section of Neuroscience and Clinical Pharmacology, Department of Biomedical Sciences, University of Cagliari, Cagliari, Italy

[8] "C. Golgi" Women Health Center, University of Brescia, 25123 Brescia, Italy

Introduction

Dopamine (DA) D2 and D3 receptors (D2R/D3R), which belong to the D2-like receptor family, are expressed on DA neurons of the substantia nigra (SN) and ventral tegmental area (VTA) [1] where they act as autoreceptors, regulating both phasic and tonic DA release [2–5]. At the molecular level, D2R/D3R are coupled to the Galphai/o family of G

proteins leading to inhibition of adenylyl cyclase (AC) [6]; in addition, D2-like receptors also regulate other intracellular signals, including the extracellular-signal-regulated kinases 1/2 (ERK1/2) pathway [7].

There is now increasing evidence that D2R/D3R is also critical for supporting DA neuron homeostasis [8]. In particular, the role of DA, via stimulation of D2R/D3R, in the regulation of proliferation and differentiation of neuronal progenitors during brain development [9–11] and in the adult rodent brain [12–14] has been described. Furthermore, a role of D2R/D3R in supporting DA neuron neurotrophic changes, which require the activation of the phosphatidylinositol 3-kinase (PI3K)/ERK1/2 pathway [15], has been demonstrated in mouse primary neuronal cultures [16]. The observation that structural changes induced by the D2R/D3R agonist quinpirole in DA neurons were lost in primary DA neurons obtained from both D2R-knockout (D2R-KO) [17, 18] and D3R-KO mice [16] suggests that both D2R and D3R contribute to these effects. D2R/D3R stimulation also protects DA neurons against neurodegenerative processes involved in the progressive loss of DA neurons of the SN in Parkinson's disease (PD). In particular, a randomized, controlled trial in PD patients has shown that the D2R/D3R agonist ropinirole slowed the progression of neurodegeneration compared with levodopa [19]. Similarly, in the 6-hydroxydopamine (6-OHDA)-lesioned rat model of PD, chronic exposure to the D2R/D3R agonist 7-hydroxy-*N*,*N*-dipropylaminotetralin (7-OHDPAT) restored the nigrostriatal pathway and improved locomotion [20]. Interestingly, using a neuroblastoma cell model, D2R/D3R stimulation has been reported to counteract glucose deprivation (GD)-induced aggregation of alpha-synuclein (alpha-syn) [21], the major component of the Lewy bodies in PD [22].

To date, the evidence that D2R/D3R share these properties in human DA neurons is still lacking. Therefore, in this study, we performed a comprehensive characterization of D2R/D3R expressed by human DA neurons derived from induced pluripotent stem cells (hiPSCs) that could provide new approach for understanding the pathogenic mechanisms underlying neurologic and neuropsychiatric diseases involving the DA system. In fact, the generation of hiPSCs [23, 24] has opened the possibility to produce neurons from patients, providing the unique opportunity for directly analyzing the mechanisms of diseases at the cellular and molecular level. DA neurons have been already derived from hiPSC and characterized for the expression of typical DA markers [25, 26] and for their electrophysiological properties [27]. However, whether these neurons are authentic DA neurons expressing the proper complement of receptors and responding to stimulation by activating the characteristic signaling effectors and functions has not been investigated.

In this study, we derived hiPSC from human healthy dermal fibroblasts and differentiated these cells into midbrain DA (mDA) neurons with the aim of investigating their molecular and functional properties in terms of D2R/D3R and other receptors expression and function. The impact of D2R/D3R stimulation on differentiation of hiPSC into mDA neurons as well as the D2R/D3R ability to inhibit DA release and to support DA neuron neuroplasticity and neuroprotection was particularly investigated. The results show that mDA neurons derived from hiPSC have a gene and protein complement typical of authentic, terminally differentiated DA neurons.

Materials and Methods

Chemicals

Ascorbic acid (AA) and adenosine-3′,5′-cyclic monophosphate (cAMP) were purchased from Sigma-Aldrich; LDN193189 and CHIR99021 (CHIR) were purchased from Stemgent (Cambridge, MA); Y27632 dihydrochloride (ROCK inhibitor) and SB431542 were purchased from Tocris Bioscience; small molecule activators of sonic hedgehog C25II (Shh), fibroblast growth factor 8 (FGF8), basic fibroblast growth factor (bFGF), brain-derived neurotrophic factor (BDNF), glial cell line-derived neurotrophic factor (GDNF), and transforming growth factor type β3 (TGFβ3) were purchased from R&D Systems (Minneapolis, MN).

Astrocytes Culture

Primary mouse cortical astrocytes (MCA) were isolated from CD1 mice at post-natal day 1 (P1) (Charles River Laboratories, Calco, Italy). Animal care was in accordance with the European Community Council Directive, September 2010 (2010/63/EU) with the approval of the Institutional Animal Care and Use Committee of the University of Brescia, and in line with Italian law. Briefly, cortices were dissected and collected in ice-cold HBSS (EuroClone). Cell suspension was diluted with DMEM (Sigma-Aldrich) 10% FBS (EuroClone), plated on 6-cm dishes and placed in an incubator at 37°C in 5% CO_2. Medium was replaced every 3–4 days.

Neural Induction

Human iPSC (hiPSC) cultures were disaggregated using Accutase (Innovative Cell Technologies) for 20 min, washed using hES medium, and pre-plated on 0.1% gelatin (Stem Cell Technologies) for 1 h at 37°C to remove mouse embryonic fibroblast (MEF) feeders, in the presence of 10-μM ROCK inhibitor (Y-27632). The non-adherent hiPSC were washed and plated at a density of 10,000–25,000 cells/cm^2 on Matrigel (BD)-coated dishes in MEF-conditioned hES

medium supplemented with 10 ng/ml of bFGF and ROCK inhibitor.

For midbrain DA neuron (mDA) induction, a modified version of the dual-SMAD inhibition protocol was used [26]. hiPSCs were cultured in knockout serum replacement medium (KSR medium) including KO-DMEM, 15% KSR, 1% P/S, 2 mM glutamine, 1% NEAA, and 0.055 mM 2-mercaptoethanol (all by Life Technologies) with 10 μM SB431542 and 100 nM LDN193189. Upon day 5, KSR medium was gradually shifted to N2 media, consisting in DMEM-F12, 1% P/S, 1% GlutaMAX, 0.2% D-Glucose, and 1% N2 supplement (GIBCO); the SB431542 was withdrawn, while LDN193189 was maintained until day 11. One hundred nanograms per milliliter of the small molecule activators of sonic hedgehog (Shh) and 100 ng/ml FGF8 were added from day 1 until day 7, while 3 μM CHIR was added from days 3 to 12. From day 11 to day 20, DA maturation was performed in the presence of 20 ng/ml BDNF, 0.2 mM ascorbic acid, 20 ng/ml GDNF, 1 ng/ml TGFβ3, and 0.5 mM cAMP (BAGTC) in Neurobasal/B27/glutamine containing medium (NB27 medium). On day 20, cells were dissociated using accutase and replated at density of 5×10^4 cell/cm^2 on polyornithine (15 μg/ml)/laminin (1 μg/ml)/fibronectin (2 μg/ml) (all from Sigma-Aldrich) pre-coated dishes or on MCA in differentiation medium (NB27 medium + BAGTC) until day 50. In order to evaluate the role of D2R/D3R during the differentiation protocol, hiPSCs (day 0) were exposed for 20 days to quinpirole (10 μM), sulpiride (5 μM), or quinpirole in combination with sulpiride, with each compound added to fresh medium every other day.

RNA Isolation and Gene Expression Analysis

Total RNA was extracted from cells during differentiation at days 0, 11, and 50, and from MCA using TriZol Reagent (Life Technologies). RNA was quantified using the My Spect spectrophotometer (Biomed). For each sample, 1 μg of total RNA was treated with DNase I and reverse-transcribed using High-Capacity cDNA Reverse Transcription kit from Life Technologies (Foster City, CA) according to the manufacturer's protocol using a thermo cycler (Applied Biosystems) at 25°C for 10 min, 37°C for 120 min, and 85°C for 5 min. RT-PCR was performed using the DreamTaq Green PCR Master Mix according to the manufacturer's instruction (Thermo Fisher).

Quantitative RT-PCR (qPCR) was performed using Sybr® Green Master Mix (Bio-Rad) and 20 ng of cDNA in triplicate for each gene and run on ViiA7 instrument (Applied Biosystems) under the following conditions: 95°C for 10 min for 1 cycle, 95°C for 15 s and 60°C for 1 min for 40 cycles.

Transcript levels of glyceraldehyde 3-phosphate dehydrogenase (GAPDH) were measured as endogenous controls. Gene expression was analyzed based on the delta CT (ΔCT) approach and normalized to the expression of GAPDH.

Primer sequences, annealing temperatures, and PCR product sizes are listed in supplementary materials (Supplementary Table S1).

Pharmacological Treatments

For biochemical analysis, cultures at day 50 of differentiation were maintained in B27-free medium for 6 h following by treatment for 2 min with the D1R agonist SKF81297 (10 μM), the D2R/D3R agonists quinpirole and ropinirole (both at 10 μM) and with DA (1 μM) and analyzed for ERK1/2 phosphorylation (pERK1/2). In addition, cells were treated with quinpirole for 2 min in the presence or in the absence of the D2R/D3R antagonist sulpiride (5 μM) or the PI3K inhibitor LY2940022 (10 μM), both added 30 min prior quinpirole stimulation. Proteins were extracted and analyzed by western blot as described below.

For morphological analysis, cultures at the 50th day of differentiation were treated with quinpirole (10 μM) or nicotine (10 μM) for 72 h both in the absence or in the presence of either sulpiride (5 μM) or the PI3K inhibitor LY2940022 (10 μM). On the basis of preliminary experiments, quinpirole and nicotine were added once at the beginning of the experiment; sulpiride and LY 2940022 were added 30 min before agonists and left in the cultures until the end of the experiment. Morphological analysis was conducted by immunocytochemistry (ICC) as described below.

In GD experiments, mDA neurons (day 50) were incubated in Hank's balanced salt solution (HBSS, Euroclone) supplemented with 2 mM glutamine and 2% B27 without glucose for 60 min at 37°C. Quinpirole (10 μM) or nicotine (10 μM) were added immediately after GD in the presence or in the absence of sulpiride (5 μM), added 30 min before agonists. Cells were divided into two groups and analyzed for alpha-synuclein (alpha-syn) aggregation (48 h after GD) and for morphological changes (both 48 and 120 h after GD).

Immunocytochemistry, Immunofluorescence, and Morphometric Analysis

For immunofluorescence (IF) analysis, cells were fixed in phosphate-buffered saline (PBS) containing 3% paraformaldehyde (Sigma-Aldrich)/3% sucrose (Sigma-Aldrich), blocked in PBS containing 0.1% Triton X-100 (Promega, Madison, WI, USA), 5% bovine serum albumin (BSA; Sigma Aldrich), and incubated overnight at 4°C with primary antibodies. The following antibodies were used: PAX6 (1:250; Covance), Nestin (1:100; Chemicon), Lmx1α (1:1000; Sigma Aldrich), FoxA2 (1:500; Santa Cruz), tyrosine hydroxylase (TH, 1:700; Santa Cruz Biotechnology), MAP2 (1:500; Millipore), dopamine transporter (DAT, 1:400; Santa

Cruz Biotechnology), and norepinephrine transporter (NET, 1:400; Santa Cruz Biotechnology) (Supplementary Table S2). Cells were then incubated for 30 min at room temperature with appropriate Alexa Fluor 488- and Cy3-conjugated secondary antibodies (Jackson Immuno Research). Nuclei were stained with DAPI. Coverslips were mounted with Vectashield Mounting Medium (Vector Laboratories). As a negative control, the primary antibodies were omitted. Images were captured using an Olympus IX51 microscope (Hamburg, Germany), or using a Zeiss LSM 510 Meta confocal microscope equipped with Plan-Apochromat 63X/1.4 numerical aperture oil objective and LSM 510 Meta Software, version 3.5 (Carl Zeiss AG, Oberkochen, Germany). Confocal digital images were further examined using the Axio Vision Release, version 4.8.2, software (Carl Zeiss AG). TH-, MAP2-, FoxA2-, and Lmx1α-positive neurons were counterstained with DAPI and counted by a blinded examiner using a ×20 objective and a cast grid system under an inverted microscope (Olympus IX51). More than 50 frames for each coverslip were examined.

Alpha-syn aggregation was analyzed by IF using the alpha-syn 211 (1:500; Santa Cruz) and the TH (1:700; Santa Cruz) (Supplementary Table S2) primary antibodies as described below. Nuclei were stained with DAPI. Alpha-syn quantification was performed as described by Zaltieri et al. [28]. A minimum of ten fields containing TH-positive neurons for each condition were selected and analyzed by using the NIH IMAGE J Software (NIH, Bethesda, MD, USA). The threshold setup was fixed between 30 and 200. The densitometric analysis is indicative of the percent average size of the alpha-syn-positive areas in the different fields analyzed. For image analysis, each experimental condition was performed in triplicate at least three times. Morphological analysis was conducted by ICC as described below.

For ICC, cells were stained with the anti-TH primary antibody as described above, followed by a biotinylated secondary antibody (Vector) and visualized via DAB chromogen. Digital images were acquired with the Olympus IX51 microscope connected to an Olympus digital camera and a PC and analyzed as previously described [16]. Morphometric measurements were performed by a blinded examiner on digitalized images using NIH ImageJ software (NIH, Bethesda, MD, USA). The morphological indicators of structural plasticity were (i) the maximal primary dendrite length, (ii) the number of dendrites, and (iii) the soma area [29]. Two coverslips per treatment were examined to obtain measurements from at least 50 TH-positive mDA neurons.

Endogenous DA Release from hiPSC-Derived Dopaminergic Neurons and HPLC Analysis

At day 50 of neuronal differentiation, the medium was removed and cells were washed twice with Krebs Ringer's buffer (KRB) containing 119 mM NaCl, 2.5 mM KCl, 2.5 mM $CaCl_2$, 1.3 mM $MgSO_4$, 1 mM NaH_2PO_4, 26.2 mM $NaHCO_3$, and 10 mM glucose at pH 7.4. Three hundred microliters of KRB were added to the cells and immediately collected (T0). Cells were then treated with 300 μl KRB (basal), or K^+ (50 mM in KRB), or nicotine (10 μM in KRB) or quinpirole (10 μM in KRB). Another group of cells was treated with nicotine in the presence of quinpirole (both at 10 μM in KRB) with quinpirole added 30 min before nicotine stimulation. All the experiments were carried out in the presence of the DAT inhibitor GBR 12935 (30 nM) to prevent DA reuptake. The medium was collected after a 30-min incubation (T30) and placed on ice and protect from light. Samples (11 μl) were injected into the HPLC apparatus. Measurements of dopamine and metabolites were made by HPLC with an electrochemical detection system (ALEXYS LC-EC; Antec Leyden BV) equipped with a reverse-phase column (3-μm particles, ALB-215 C18, 1 × 150 mm; Antec Leyden BV) at a flow rate of 50 μl/min and electrochemically detected by a 0.7-mm glass carbon electrode (VT-03; Antec Leyden BV). The mobile phase contained 50 mM H_3PO_4, 50 mM citric acid, 8 mM KCl, 0.1 mM EDTA, 400 mg/l octanesulfonic acid sodium salt and 8% (v/v) acetonitrile (pH 3.0).

Western Blotting

mDA neuron cultures were washed with ice-cold PBS and lysed in 50 mM Tris (pH 7.4) containing 150 mM NaCl, 0.5% sodium deoxycholate, 0.1% sodium dodecyl sulfate, 1% Igepal, 1 mM polymethanesulphonyl fluoride, and a complete set of protease inhibitors (Roche Diagnostics, Mannhein, Germany). Protein concentration was measured with a DC-protein assay (Bio-Rad, Hercules, CA, USA). Aliquots of total proteins were resolved by 10% sodium dodecyl sulfate polyacrylamide gel electrophoresis and blotted onto a PVDF membrane (Immobilon-P; Millipore). Membranes were incubated overnight with the following primary antibodies: pERK1/2 (1:1000; Santa Cruz Biotechnology), TH (1:1000; Millipore), DAT (1:400; Santa Cruz Biotechnology), AADC (1:200; Sigma-Aldrich), and α-Tubulin (1:100,000; Sigma-Aldrich) (Supplementary Table S2). Blots were then incubated with the appropriate horseradish peroxidase-conjugated secondary antibodies (Santa Cruz Biotechnology) and developed using ECL (Gene Spin). Specific bands were analyzed by densitometric scanning of exposed film using gel-pro analyzer software (Media Cybernetics, Bethesda, MD, USA).

Statistical Analysis

Each experiment was repeated at least three times. Values are expressed as mean ± standard error of the mean (S.E.M.) if not

stated otherwise. Significant differences from control conditions were determined using analysis of variance (ANOVA) followed by Bonferroni's test for multiple comparisons provided by GraphPad prism version 4.00 for Windows (GraphPad Software, San Diego, CA, USA). Correlations were assessed by calculating the correlation coefficient between two variables using the same statistical package.

Results

Induction and Neurogenic Conversion of hiPSCs into mDA Neurons

hiPSCs were generated from healthy fibroblasts as described in supplementary data (Fig. S1) following the protocol published by Maherali et al. [30] and differentiated into mDA neurons using a modified version of the dual-SMAD inhibition protocol developed by Kriks et al. [26]. Gene expression analysis for markers of pluripotency (day 0), neural progenitors (day 11), or mDA neurons (day 50) was performed during the differentiation process by semiquantitative RT-PCR. As shown in Fig. 1b, at day 0, hiPSCs expressed the mRNAs encoding for the endogenous pluripotency genes, OCT4 and SOX2; in line with other studies [11], the mRNA encoding for DA D2R, D3R, and D4R was also detected at day 0. The mRNAs for the neural progenitors genes PAX6 and Nestin were robustly induced at day 11; the transcript encoding for the microtubule-associated protein 2 (MAP2), a well-recognized neuronal marker [31], was also identified at day 11. The mRNA for genes typical of DA neurons, such as tyrosine hydroxylase (TH), aromatic amino acid decarboxylase (AADC), DA transporter (DAT), and vesicular monoamine transporter (VMAT2), was expressed starting from day 11 of differentiation. The mRNA encoding for the G protein-coupled inwardly rectifying potassium channel, GIRK2, a marker of A9 DA neurons, was also detected at both days 11 and 50 of differentiation. Moreover, the transcripts encoding for several DA neurons transcription factors, such as Lmx1α, FoxA2, Nurr1, and Pitx3, detected starting from day 11, were greatly increased at day 50 of differentiation.

The mRNA for glutamic acid decarboxylase 67 (GAD67), vesicular glutamate transporter 2 (V-GLUT2), norepinephrine and serotonin transporters (NET and SERT, respectively), and the serotonin receptor 2C (5-HT2C) was also identified (Fig. 1b), suggesting that in addition to DA neurons, GABAergic, serotonergic, glutamatergic, and noradrenergic neurons also coexist in our cultures.

The neural progenitor markers PAX6 and Nestin, as well as the transcription factors Lmx1α, FoxA2, were also evaluated at day 11 by immunocytochemistry (Fig. 1c). The majority of cells expressed both PAX6 and Nestin thus indicating their differentiation toward neuronal precursors (Fig. 1c (a–c)). Moreover, a high percentage of cells expressed Lmx1α and FoxA2 (Fig. 1c (d–f)), with ~75% co-expressing both transcription factors, suggesting the DA neuron precursors predominance in the cell cultures (Fig. 1c (g)). MAP2 and TH were also examined at day 50 (Fig. 1d (a–c)). The majority of cells were positive for the neuronal marker MAP2 (~82% of the cells), and ~40% of cells co-expressed TH and DAT (Fig. 1d (d–h)). Only a small cluster of TH-positive neurons was also positive for NET staining thus indicating the presence of a small population of noradrenergic neurons in the culture (Fig. 1d (i–k)). The expression of TH, AADC, and DAT was also detected by WB in lysates obtained at day 50 (Fig. 1e).

Functional Characterization of Differentiated mDA Neurons

To determine whether mDA neurons, at day 50 of differentiation, synthesize and release DA in a regulated way, HPLC was used to measure endogenous DA levels in the culture medium both in basal conditions and following stimulation of D2R/D3R and nicotinic acetylcholine receptors (nAChR), which are known to control of DA release [6, 32, 33]. The transcripts encoding for D2R and D3R and for both the α4/α6 and β2 subunits of nAChR [33] were in fact detected in mDA neurons at day 50 by RT-PCR (Figs. 1b and 2a). mDA neurons were treated with either potassium (K^+; 50 mM) [34], nicotine (10 μM) [35], quinpirole (10 μM), or with nicotine in combination with quinpirole (both at 10 μM), in the presence of the DAT blocker GBR12935 (30 nM) [36]. DA content in the culture medium was measured after a 30-min stimulation.

As shown in Fig. 2b, both nicotine and K^+ significantly increased DA release (0.511 ± 0.04 ng/ml and 0.800 ± 0.25 ng/ml, respectively) as compared to basal conditions (0.267 ± 0.006 ng/ml). Quinpirole, which did not modify basal DA release (0.272 ± 0.011 ng/ml), significantly inhibited nicotine-induced DA release (0.232 ± 0.013 ng/ml). Overall, these data suggest that mDA neurons synthesize and release DA and that this effect is precisely regulated by the activation of functional D2R/D3R and nAChR.

Involvement of D2R/D3R in mDA Neurons Differentiation

The involvement of D2R/D3R in hiPSC differentiation into mDA neurons was analyzed [11, 13, 17, 18, 37–39]. To this aim, either the D2R/D3R agonist quinpirole (10 μM) or the D2R/D3R antagonist sulpiride (5 μM) was added to hiPSC cultures from day 0 (pluripotent cell stage) and maintained in the cultures to day 20 (Fig. 3a). Cells were analyzed at day 20 for MAP2 and TH immunoreactivity. Quinpirole increased the number of both MAP2- and TH-positive neurons (33 and 23% increase, respectively); by contrast, the percentage of MAP2- and TH-positive neurons was significantly decreased by

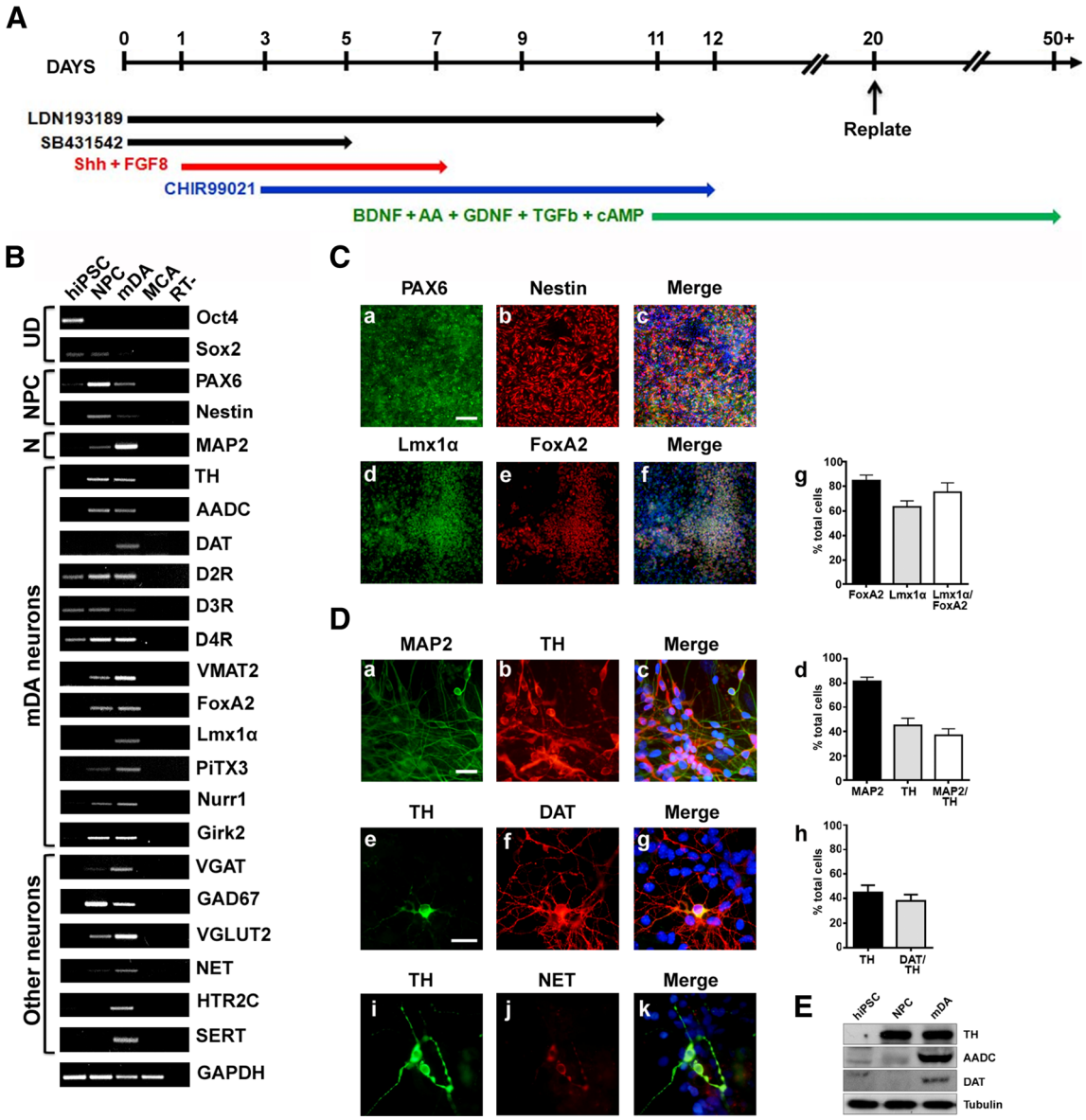

Fig. 1 In vitro maturation and characterization of midbrain DA (mDA) neurons. **a** Time scheduled and culture condition of hiPSC differentiation into mDA neurons. **b** The expression of markers typical of the undifferentiated cells (*UD*), the neural progenitors cells (*NPC*), or the mDA neurons (*mDA*) was analyzed by using RT-PCR in hiPSC (day 0), in NPC (day 11), in mDA neurons (day 50), or in mouse cortical astrocytes (*MCA*). Analysis of GAPDH mRNA was used as endogenous control. **c** Immunofluorescence analyses of PAX6 (*a*), Nestin (*b*), and co-staining (*c*) at day 11; immunofluorescence of Lmx1α (*d*), FoxA2 (*e*), and co-staining (*f*); Lmx1α- and FoxA2-positive cells were counted as described in "Materials and Methods." *Bars* referred to panel *d–f* represent the mean ± S.E.M of three independent experiments (*g*). *Scale bar* = 100 μm. **d** Immunofluorescence analyses of MAP2 (*a*), TH (*b*), and co-staining (*c*) in mDA neurons at day 50. MAP2- and TH-positive cells were counted. *Bars* referred to panel *a–c* represent the mean ± S.E.M. of three independent experiments (*d*). Immunofluorescence analyses of TH (*e*), DAT (*f*), and co-staining (*g*) in mDA neurons at day 50. DAT- and TH-positive cells were counted. *Bars* referred to panels *e–g* represent the mean ± S.E.M. of three independent experiments (*h*). Immunofluorescence analyses of TH (*i*), NET (*j*), and co-staining (*k*) in mDA neurons at day 50. Nuclei were stained with DAPI (*blue*). *Scale bar* = 50 μm. **e** Western blot (WB) analysis of TH, AADC, DAT, and tubulin in hiPSC (day 0), NPC (day 11), and mDA neurons (day 50)

sulpiride (27 and 17% decrease, respectively) (Fig. 3b). The increase of both MAP2- and TH-positive neurons induced by quinpirole was lost when quinpirole was added to cultures in combination with sulpiride (5 μM) from day 0 (Fig. 3b).

Since D2-like receptors may be implicated in these mechanisms [11], D2R, D3R, and D4R mRNA expression was analyzed by quantitative RT-PCR (qPCR) during hiPSC maturation to mDA neurons. Low to moderate levels of the mRNA encoding for D2R (ΔCt 12.34 ± 0.23), D3R (ΔCt 12.86 ± 0.39), and D4R (ΔCt 9.42 ± 0.13) were detectable in hiPSC, while the mRNA encoding for TH was almost absent (ΔCt 15.67 ± 0.04). During differentiation, the mRNAs

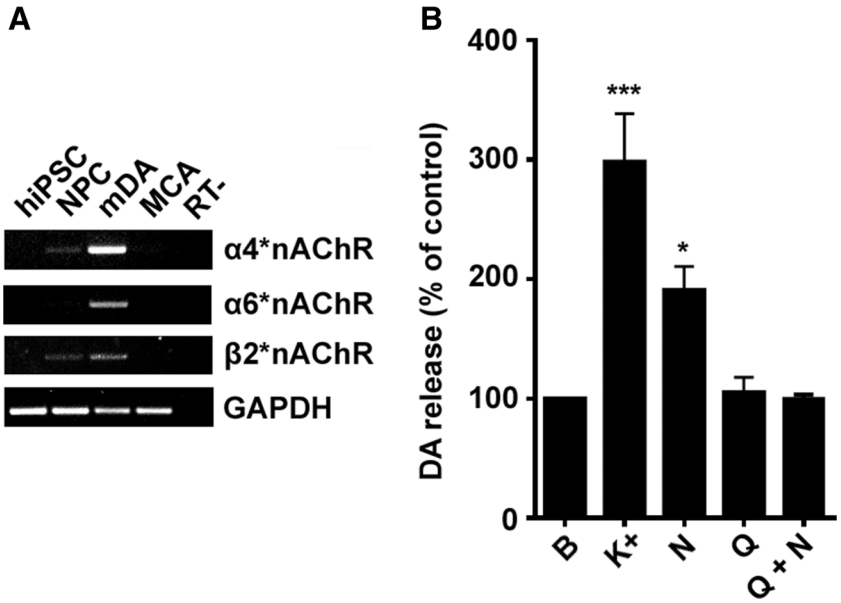

Fig. 2 Functional DA release in hiPSC-derived mDA neurons. DA release by mDA neurons was determined by using HPLC, as described in "Materials and Methods." **a** RT-PCR analysis of mRNA encoding for both α4/α6 and β2 subunit of nAChR in hiPSC (day 0), neuronal progenitor cells (NPC; day 11), mDA neurons (day 50), and MCA. Analysis of GAPDH mRNA was used as endogenous control. **b** mDA neurons were stimulated with potassium (K+; 50 mM), nicotine (N; 10 μM), quinpirole (Q; 10 μM), or quinpirole plus nicotine (both at 10 μM) for 30 min and analyzed as described in "Materials and Methods." Experiments were repeated at least three times. Values are represented as mean ± S.E.M. (***$p < 0.001$; $^{*}p < 0.05$ vs basal (B) release). Data were statistically analyzed by one-way ANOVA followed by post hoc comparison with Bonferroni test

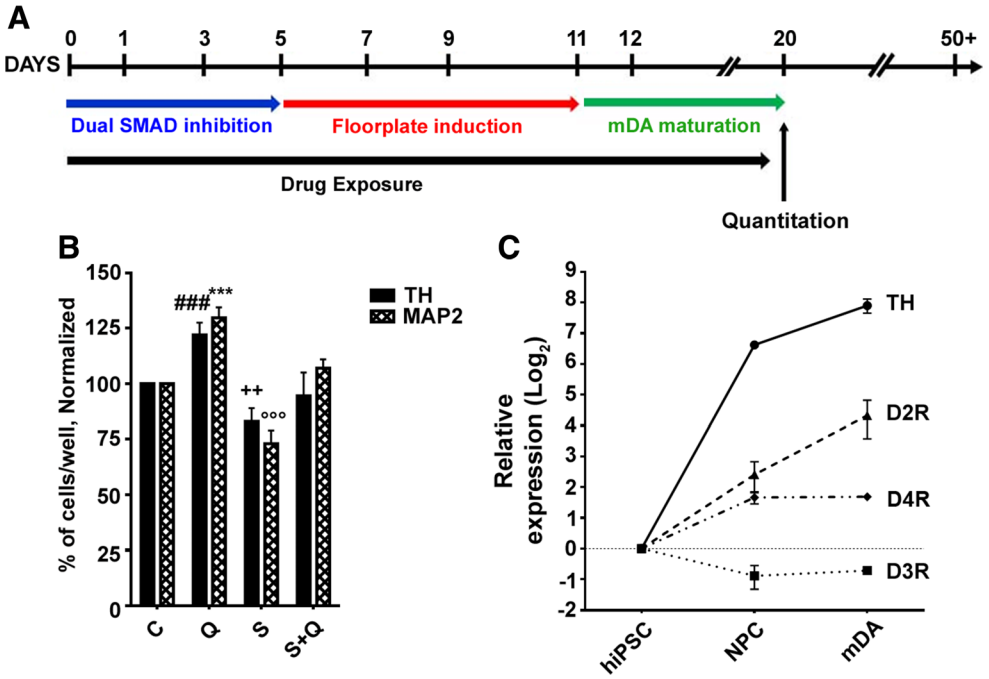

Fig. 3 Effect of D2R/D3R in the differentiation of hiPSC into mDA neurons. **a** Time scheduled and culture condition of hiPSC differentiation into mDA neurons. hiPSCs (day 0) were exposed for 20 days to quinpirole (10 μM), sulpiride (5 μM), or quinpirole in combination with sulpiride, with each compound added to fresh medium every other day. **b** At day 20 of differentiation, cells were analyzed for TH and MAP2 by immunocytochemistry and counted, as described in "Materials and Methods." Data were combined from three independent experiments. *Bars* represent the mean ± S.E.M. ***$p < 0.001$; ###$p < 0.001$; ++$p < 0.01$; °°°$p < 0.001$ vs untreated cells. Data were statistically analyzed by one-way ANOVA followed by post hoc comparison with Bonferroni test. **c** Temporal expression of the mRNA encoding for TH, D2R, D3R, and D4R analyzed by using qPCR in untreated hiPSC (day 0), NPC (day 11), and mDA neurons (day 50). Gene expression was analyzed based on the delta CT (ΔCT) approach and normalized to the expression of GAPDH (relative expression). Shown are the averages and standard deviations of three independent experiments

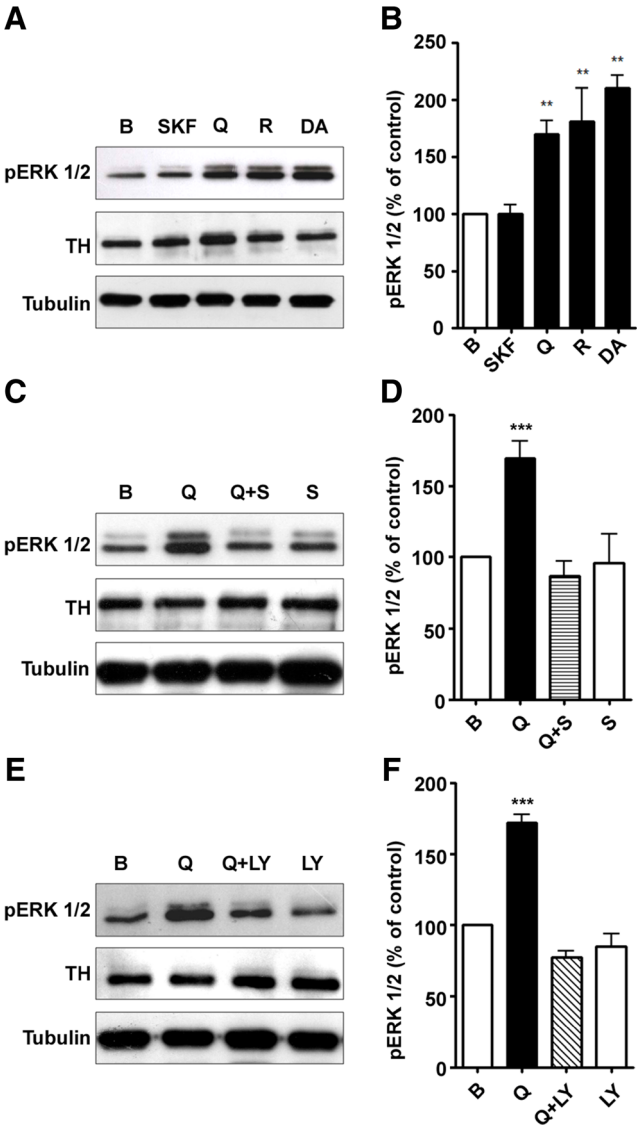

Fig. 4 D2R/D3R activation of ERK1/2 in hiPSC-derived mDA neurons. **a** mDA neurons were stimulated for 2 min with the D1R agonist SKF81297 (SKF; 10 μM), the D2R/D3R agonists quinpirole (Q; 10 μM) and ropinirole (R; 10 μM), or with dopamine (DA; 1 μM) and analyzed for ERK1/2 phosphorylation (pERK1/2) by WB. A representative WB is shown. **b** Densitometric analysis of blots (n = 4) with specific levels of pERK1/2 normalized to the corresponding TH and tubulin levels. *Bars* represent the mean ± S.E.M. $^{**}p < 0.01$ vs basal (B). **c** mDA neurons were stimulated for 2 min with quinpirole (10 μM) in the presence or absence of the D2R/D3R antagonist sulpiride (5 μM), added 30 min before treatment. A representative WB is shown. **d** Densitometric analysis of blots (n = 4) with specific levels of p-ERK1/2 normalized to the corresponding TH and tubulin levels. *Bars* represent the mean ± S.E.M $^{***}p < 0.001$ vs B. **e** mDA neurons were stimulated for 2 min with quinpirole (10 μM) in the presence or absence of the PI3K inhibitor LY294002 (LY; 10 μM), added 30 min before treatment. A representative WB is shown. **f** Densitometric analysis of blots (n = 4) with specific levels of p-ERK1/2 normalized to the corresponding TH and tubulin levels. *Bars* represent the mean ± S.E.M. $^{***}p < 0.001$ vs B. Data were statistically analyzed by one-way ANOVA followed by post hoc comparison with Bonferroni test

encoding for TH, D2R, and D4R were strongly upregulated (TH: day 11: ΔCt 8.29 ± 0.46 and day 50: ΔCt 4.58 ± 0.09; D2R: day 11: ΔCt 9.95 ± 0.21 and day 50: ΔCt 8.56 ± 0.27; D4R: day 11: ΔCt 7.65 ± 0.10 and day 50: ΔCt 7.71 ± 0.22), while D3R mRNA was slightly downregulated (day 11: ΔCt 14.63 ± 0.29; day 20: ΔCt 13.70 ± 0.45) (Fig. 3c).

Functional D2R/D3R Are Expressed on hiPSC-Derived mDA Neurons

We previously reported that stimulation of D2R/D3R in mouse primary midbrain DA neurons results in the phosphorylation of the extracellular-signal-regulated kinases 1/2 (ERK1/2) pathway, an effect mediated by PI3K [15, 16]. Evidence indicating that mDA neurons express D2R/D3R has been provided by RT-PCR and qPCR and by measuring DA release (Figs. 1b, 2b, and 3c). D2R/D3R signaling to ERK1/2 was tested in hiPSC-derived mDA neurons (day 50), cultured on murine cortical astrocytes feeders, following 5 days of culture in Neurobasal/B27 medium deprived of growth factors. Cells were treated with quinpirole (10 μM), ropinirole (10 μM), the D1R agonist SKF81297 (10 μM), and DA (1 μM) for 2 min. As shown in Fig. 4a, b, a rapid and significant increase of ERK1/2 phosphorylation was induced by quinpirole, ropinirole, and DA, as compared to untreated cells; these effects were counteracted by sulpiride (5 μM), given 30 min prior stimulation (Fig. 4c, d). By contrast, treatment with SKF81297 did not affect ERK1/2 phosphorylation. On this line, by using RT-PCR, the mRNAs for neither D1R nor D5R were detected in mDA neurons (data not shown). In parallel experiments, cultures of pure cortical astrocytes were treated with quinpirole (10 μM), ropinirole (10 μM), or DA (1 μM) for 2 min and analyzed for ERK1/2 phosphorylation. These agonists did not affect this pathway, thus indicating the irrelevance of the astrocyte feeder in investigating the signaling properties of D2R/D3R in mDA neurons (data not shown). To define the pathway involved in D2R/D3R-mediated ERK1/2 activation, mDA neurons were treated for 2 min with quinpirole (10 μM) in the presence of the PI3K inhibitor LY294002 (10 μM), given 30 min prior stimulation. LY294002 significantly prevented ERK1/2 activation induced by quinpirole (Fig. 4e–f).

D2R/D3R Stimulation Promotes the Morphological Remodeling of Human TH-Positive mDA Neurons

The ability of D2R/D3R in supporting structural plasticity of mouse mDA neurons, an effect depending on the engagement of the PI3K-ERK1/2 signaling, was recently described [16]. Interestingly, in the same cell model, functional D3R was required also for nicotine-induced structural plasticity [35], pointing to the crucial role of D2R/D3R in providing neurotrophic support to DA neurons. On this basis, we investigated whether stimulation of D2R/D3R or nAChR induces the morphological remodeling of mDA neurons derived from hiPSC. To this aim, mDA neurons (50 days of differentiation) were

cultured for 5 days in Neurobasal/B27 medium without growth factors and then were stimulated with quinpirole (10 μM) or nicotine (10 μM) for the next 72 h. mDA neurons were also treated with quinpirole (10 μM; 72 h) or nicotine (10 μM; 72 h) in combination with sulpiride (5 μM) or with the PI3K inhibitor LY294002 (10 μM) and analyzed for morphological changes. The following endpoints were used as relevant indicators of neurotrophic effects [16, 29]: (i) average maximal length of the primary dendrite, (ii) number of dendrites, and (iii) soma area. As shown in Fig. 5a, in TH-positive mDA neurons, quinpirole significantly increased the maximal length of the primary dendrite (Fig. 5b), the dendrite number (Fig. 5c), and the soma area (Fig. 5d) compared to untreated cells. Similar effects were observed with nicotine (Fig. 5b–d). The neurotrophic effects of quinpirole were specifically blocked by sulpiride (Fig. 5b–d) and LY294002 (Fig. 5b–d), suggesting the involvement of PI3K-dependent mechanisms. Interestingly, the neurotrophic effects of nicotine were also abolished by the D2R/D3R antagonist, suggesting the existence of a functional cross talk between nAChR and D2R/D3R. Sulpiride and LY294002, when administered alone, did not produce any effect on mDA neuron morphology (Fig. 5b–d).

D2R/D3R Stimulation Prevents Alpha-Synuclein Aggregation Induced by GD in TH-Positive mDA Neurons

Pathological inclusions enriched in alpha-syn in DA neurons are typically associated with PD [22]. According to previous studies [21], we induced alpha-syn aggregation in human mDA neurons by GD. In particular, mDA neurons were exposed to GD for 1 h and then cultured in the absence or in the presence of either quinpirole (10 μM) or nicotine (10 μM) for the next 48 and 120 h. Forty-eight hours after GD, TH-positive mDA neurons were analyzed for alpha-syn aggregation by immunocytochemistry. In TH-positive mDA neurons, alpha-syn was distributed in both cell body and dendrites (Fig. 6a (a–c)). GD significantly modified alpha-syn staining, as shown by the numerous dot-like inclusions into the neurons suggestive of alpha-syn aggregation (Fig. 6a (d–f), b). Remarkably, alpha-syn inclusions were drastically reduced by both quinpirole (Fig. 6a (g–i), b) and nicotine (Fig. 6a (j–l), b); these effects were significantly antagonized by sulpiride (Fig. 6a (m–o, p–r) for quinpirole and nicotine plus sulpiride, respectively; Fig. 6b). TH-positive mDA neuron structural plasticity was analyzed both 48 and 120 h following the toxic insult. While no morphological changes were

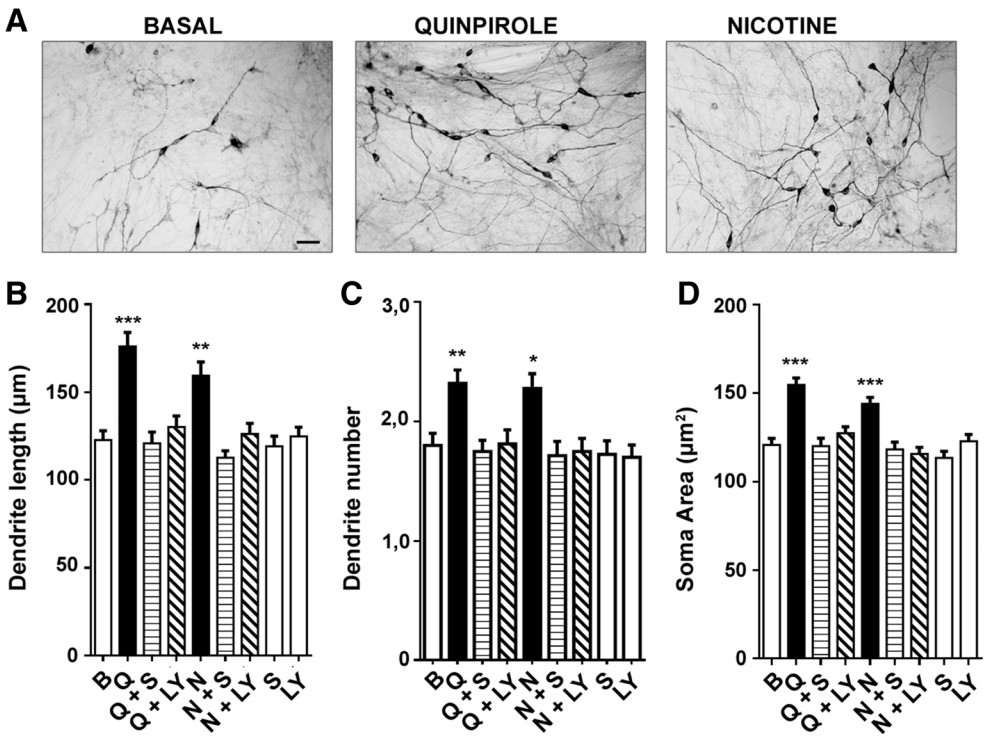

Fig. 5 Morphologic effects of quinpirole and nicotine in hiPSC-derived mDA neurons. **a** Representative microphotographs of TH-positive neurons following exposure for 72 h to quinpirole (10 μM) or nicotine (10 μM). *Scale bar* = 50 μm. **b–d** Morphologic effects of quinpirole (Q) and nicotine (N) on maximal dendrite length (**b**), number of primary dendrites (**c**), and soma area (**d**), calculated as described in "Materials and Methods." Effects of D2R/D3R antagonists sulpiride (S; 5 μM), added 30 min before quinpirole (10 μM) or nicotine (10 μM) treatment on maximal dendrite length (**b**), number of primary dendrites (**c**), and soma area (**d**). Effects of LY294002 (LY; 10 μM), added 30 min before quinpirole (10 μM) or nicotine (10 μM) treatment on maximal dendrite length (**b**), number of primary dendrites (**c**), and soma area (**d**). *Bars* represent the mean ± S.E.M. ***$p < 0.001$; **$p < 0.01$; *$p < 0.05$ vs basal (B). Data were statistically analyzed by one-way ANOVA followed by post hoc comparison with Bonferroni test

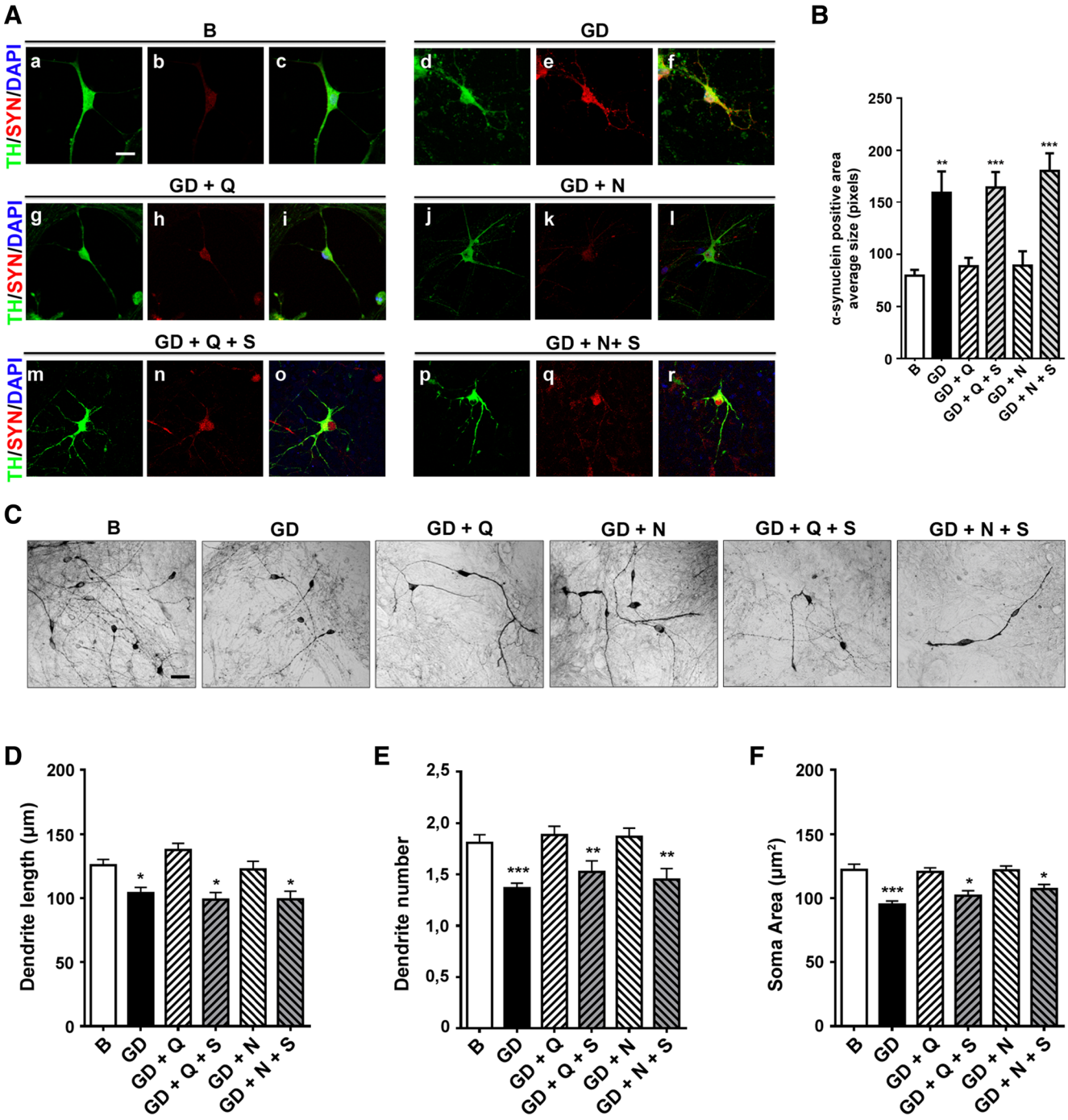

Fig. 6 Glucose deprivation (GD)-induced alpha-synuclein (alpha-syn) aggregation is counteracted by D2R/D3R and nicotine stimulation. hiPSC-derived DA neurons were exposed to GD for 1 h following by incubation with quinpirole (Q; 10 μM) or nicotine (N; 10 μM), in the absence or in the presence of sulpiride (S; 5 μM), added 30 min prior to treatment with quinpirole or nicotine. **a** Analyses of TH (*green*) and alpha-syn (SYN; *red*) in hiPSC-derived DA neurons by immunocytochemistry and confocal analysis 48 h. *Scale bar* = 20 μm. **b** Quantification of the percentage average size of the alpha-syn-immunopositive area in the different conditions analyzed at 48 h. *Bars* represent mean ± S.E.M. $^{**}p < 0.01$; $^{***}p < 0.001$ vs basal (B). Data were statistically analyzed by one-way ANOVA followed by post hoc comparison with Bonferroni test. **c** Representative microphotographs of TH-positive neurons in basal conditions (B), GD, and GD following exposure to quinpirole (Q; 10 μM), nicotine (N; 10 μM), or sulpiride (S; 5 μM) for 120 h. *Scale bar* = 50 mm. **d**–**f** Morphologic effects induced by GD and GD plus quinpirole or nicotine in the presence of absence of sulpiride on maximal dendrite length (**d**), number of primary dendrites (**e**), and soma area (**f**). *Bars* represent mean ± S.E.M. $^{***}p < 0.001$; $^{**}p < 0.01$; $^{*}p < 0.05$ vs B. Data were statistically analyzed by one-way ANOVA followed by post hoc comparison with Bonferroni test

detectable 48 h after GD (data not shown), at 120 h a significant decrease of the maximal length of primary dendrite, the number of dendrites and soma area was observed in GD-treated mDA neurons as compared to untreated cells (Fig. 6c, d–f). Quinpirole significantly counteracted GD-induced damage, restoring the primary dendrite length, the number of dendrites and soma area (Fig. 6c, d–f); similar results were obtained with nicotine (Fig. 6c, d–f). Both quinpirole and nicotine-induced restoration of morphological changes were significantly antagonized by sulpiride (Fig. 6c, d–f).

Discussion

In this paper, by using human iPSC, we have successfully recapitulated the process of midbrain neurogenesis, efficiently generating a neuronal population enriched in TH/DAT-positive mDA neurons. Authentic terminally differentiated mDA neurons were obtained from hiPSC after 50 days in culture. In particular, at day 50, the majority of hiPSC-derived cells were positive for the neuronal marker MAP2 and ~40% of these neurons co-expressed TH and DAT. Other studies reported that iPSC-derived mDA neurons may release DA in the culture media [26, 27]. We now report that mature mDA neurons release endogenous DA in a regulated way. DA release was, in fact, increased by a synaptic releaser, such as potassium and, most importantly, it was stimulated by nicotine, that is well-known to control DA release in mature rodent neurons by mainly interacting with α4α6-β2 nAChR [32, 33]. Moreover, we report that, as in the physiological systems, the release of DA induced by nicotine was blocked by quinpirole [6, 32, 33]. Thus, based on both mRNA expression and the functional interaction between nAChR and D2-like receptor in controlling DA release, it is indicated that mDA neurons generated from human iPSC co-express functional D2R/D3R and the nAChR. We have identified the mRNA for α4, α6, and β2 nAChR subunits in our cultures, suggesting that, as in other systems, this nAChR subtype is likely to be involved in the control of DA release in human iPSC-derived DA neurons. However, whether other nAChR subtypes may be involved need to be further investigated. Together, these data indicate that mDA neurons derived from hiPSC express the proper complement of nAChR and D2-like receptors controlling DA release, suggesting that they reach the full maturation.

Increasing evidence suggests that DA and D2-like receptors are required for neural differentiation during both development and neurogenesis in adult brain [11, 13, 17, 18, 37–39]. The possibility to monitor mDA neurons development during their in vitro differentiation from hiPSC represents a powerful tool for investigating the role of D2-like receptors in these processes; interestingly, the mRNAs encoding for D2R, D3R, and D4R were detected in the undifferentiated hiPSC, suggesting their susceptibility to DA already in the pluripotent state. By contrast, the mRNA for TH, which was undetectable in this stage, was strongly upregulated at later stages suggesting that early, during the differentiation protocol, hiPSC-derived neuronal progenitors acquire the property to produce and release DA. In this study, we found that the number of both MAP2- and TH-positive neurons was increased by quinpirole, an effect significantly counteracted by the D2R/D3R receptor antagonist sulpiride, when given in combination with quinpirole. On the other hand, sulpiride, when given alone, significantly impaired the proliferation of MAP2- and TH-positive neurons. Although an improvement in the yield of other hiPSC-derived neurons, such as the GABAergic or glutamatergic neurons, has not been investigated, our data suggest that the role of D2-like receptors is to selectively amplify the multipotent/neuronal progenitor cell population before differentiation toward specific neuronal phenotypes [11]. Intriguingly, while D2-like receptors stimulation decreases cAMP levels, a cAMP supplement is currently used for DA neurons differentiation [11, 40]. Therefore, it is likely that additional D2-like receptors-induced intracellular events, as for example ERK1/2 activation, can modulate neuronal proliferation [11, 18].

The PI3K/ERK1/2 signaling pathway has been shown to sustain D2R/D3R-mediated morphological changes in primary rodent neuronal cultures [16, 41, 42]. We demonstrate here that in hiPSC-derived mDA neurons, D2R/D3R stimulation by quinpirole transiently activated the ERK1/2 pathway. In addition, a chronic treatment with quinpirole led to a significant remodeling of both dendritic arborization and soma size of TH-positive DA neurons, an effect likely dependent on the ERK cascade. The requirement of ERK1/2 activation in several neuronal processes, including the structural plasticity, has been previously described [15, 16, 41–43]. However, whether a persistent activation of ERK1/2 is required for sustaining neurotrophic effects or whether a transient activation of this pathway is sufficient for triggering subsequent cellular responses leading to morphological changes of TH-positive neurons remains to be investigated.

The individual role of D2R and D3R in exerting the neurotrophic effects on mDA neurons is hardly to define due to the lack of selective ligands. Based on mRNA analysis, mDA neurons at day 50 express both D2R and D3R, with the D2R expressed at higher levels than the D3R. Interestingly, data obtained from D2R- and D3R-KO mice suggested that both D2R and D3R are necessary to provide neurotrophic support to DA neurons [15–17, 35]; therefore, even if expressed at low levels, the D3R likely provides a crucial contribution to D2-like agonist-induced neurotrophic effects on mDA neurons.

A moderate level of mRNA encoding for D4R was also measured in mDA cultures. However, according to the main localization of this receptor at the post-synaptic sites of

GABAergic neurons of several brain areas [44–46], the D4R should be mostly localized in other neuronal phenotypes present in our cultures and its contribution to the morphological remodeling of TH-positive DA neurons is unlikely.

Exposure to nicotine significantly supported TH-positive DA neuron structural modifications, increasing both the dendritic complexity and the soma area. The involvement of D2R/D3R in nicotine-induced neurotrophic effects was suggested by the observation that sulpiride counteracted nicotine-induced morphological changes. This observation is in line with previous studies in knockout mouse models demonstrating that functional D3R are required for the neurotrophic effects of nicotine in DA neurons [35].

The simplest explanation of this observation is that DA, released in response to nicotine, by activating D2R/D3R, promotes the morphological remodeling of TH-positive neurons and protects against toxic stimuli. Other mechanisms, however, can be involved in the functional cross talk between D2R/D3R and nAChR including either the convergence of their signaling pathways or transactivation mechanisms or the formation of heteromeric complexes. In particular, one of the properties of G protein-coupled receptors (GPCR) is their propensity to physically associate with both closely related and structurally-divergent receptors, as ligand-gated ion channels, to generate heteromers with peculiar properties, suggesting that heteromerization represents a key integrative mechanism at neuronal level. Receptor heteromers formed by DA D1R and glutamate NMDAR [47] and DA D5R and GABA-AR [48] have been in fact identified and characterized. On this line, it has been suggested that the existence of a D2R-nAChR heteromer controlling DA release [49] and preliminary data obtained in our laboratory strongly suggest that the D3R may directly interact with the nAChR. Formation of receptor heteromers could thus contribute to the functional interactions between D2R/D3R and nAChR in iPSC-derived TH-positive neurons. Further studies will be carried out in the future to clarify this point.

Thus, the D2R/D3R-induced neurotrophic effects could explain the neuroadaptive potential typical of DA neurons in response to different stimuli. In particular, it is well accepted that changes in neuron morphology, at the dendrites and dendritic spines, contribute to the molecular mechanisms relevant for addiction disorders [50, 51]. On this line, nicotine, the main agent delivered through tobacco smoking, is an addictive compound [52]; on the other hand, chronic administration of D2R/D3R agonists, currently used for both PD therapy and for other disorders, such as restless leg syndrome and prolactin-secreting pituitary tumors [53], has been associated with the development of a heterogeneous group of addictive behaviors [53, 54]. Thus, in hiPSC-derived mDA neurons, the structural changes exerted by quinpirole and nicotine, via D2R/D3R signaling, could represent the abnormal maladaptive morphological event that might contribute to the development of addiction.

Besides providing evidence for a role of D2R/D3R in supporting human mDA neuronal trophism, a specific role of these receptors in neuronal protection has been also documented. Immunochemistry has shown that hiPSC-derived mDA neurons express alpha-syn, thus representing a useful in vitro model for analyzing the neurodegenerative events underlying PD. It is well accepted that alpha-syn aggregation is closely associated with the neurodegenerative processes of DA neurons in PD [22]. We demonstrated that in TH-positive mDA neurons, energy starvation induced by GD leads to aggregation of alpha-syn into inclusions detected throughout the cell bodies and dendrites. These inclusions, observed 48 h after the toxic insult, were associated with alteration of the TH-positive neurons morphology. Interestingly, alpha-syn aggregation was prevented by stimulation of D2R/D3R immediately after GD. It is believed that improper activity of the ubiquitin-proteasome system (UPS) leading to impaired removal of misfolded proteins is critical for degenerative processes leading to PD [55]. Intriguingly, in a mouse model of PD with impaired UPS activity, administration of pramipexole, an agonist of D2R/D3R commonly used in PD disease [56], exerted neuroprotective effects on DA neurons by restoring the proteasomal activity [57]. As shown for remodeling effects, the requirement of either D2R or D3R or both in protecting DA neurons from toxic insult has not been defined.

Increasing evidence suggests that nicotine exerts neuroprotective effects against DA neuron neurodegeneration through several potential mechanisms counteracting oxidative stress and neuroinflammation [58]. Moreover, in vitro studies demonstrated a direct ability of nicotine to inhibit the formation of alpha-syn aggregates [59, 60]. Here, we demonstrated that in hiPSC-derived mDA neurons, chronic treatment with nicotine efficiently counteracted alpha-syn aggregation induced by GD. It is important to note that quinpirole and nicotine counteracted both the formation of alpha-syn aggregates induced by GD and the associated structural alterations. Remarkably, the effects of both compounds were significantly blocked by the D2R/D3R antagonist sulpiride, suggesting the possibility that, as shown for the remodeling effects, nAChR and D2R/D3R could cooperate for preventing alpha-syn aggregation and the morphological damages.

Both D2R/D3R agonists, such as pramipexole, and nicotine have been considered as disease-modifying drugs for PD [61]. However, recent clinical trials in PD patients did not support pramipexole as a disease-modifying agent, while those for nicotine are currently in progress [61]. Given that the formation of insoluble aggregates of alpha-syn is likely an early and irreversible process [62, 63], there is a possibility that D2R/D3R stimulation would be unable to counteract the aggregation once it has been occurred.

In conclusion, in this study, we characterized, for the first time, human mDA neurons generated from iPSC in terms of regulated DA release, expression, transductional properties

and function of D2R/D3R, and their interaction with the nAChR. We provided evidence that D2R/D3R are crucially involved in mDA neurons development, morphological plasticity, and protection thus indicating that abnormal D2R/D3R function may be associated with DA neurons vulnerability. On this line, investigating the D2R/D3R properties in patient-derived mDA neurons may unveil molecular pre-degenerative alterations that could critically contribute to the pathogenesis of brain diseases involving the DA system such as PD.

Acknowledgements We thank Ginetta Collo and Laura Cavalleri for their contribution in hiPSC generation, and Lee L. Rubin and Eunju Chung for helping in the development of midbrain DA neurons differentiation. We are also grateful to Konrad Hochedlinger for plasmids located in the Addgene depository.

Compliance with Ethical Standards

Funding This work was supported by "C. Golgi" Foundation, Brescia, Italy.

Conflict of Interest The authors declare that they have no conflict of interest.

Ethics Approval Informed consent was obtained from a healthy donor prior to cell donation. The local ethics committee (CEIOC—Fatebenefratelli Hospital "San Giovanni di Dio" – Brescia, Italy, 44/2001 and 39/2005), previously approved this consent form.

References

1. Diaz J, Pilon C, Le Foll B, Gros C, Triller A, Schwartz JC, Sokoloff P (2000) Dopamine D3 receptors expressed by all mesencephalic dopamine neurons. J Neurosci 20:8677–8684
2. De Mei C, Ramos M, Iitaka C, Borrelli E (2009) Getting specialized: presynaptic and postsynaptic dopamine D2 receptors. Curr Opin Pharmacol 9(1):53–58. doi:10.1016/j.coph.2008.12.002
3. Sokoloff P, Diaz J, Le Foll B, Guillin O, Leriche L, Bezard E, Gross C (2006) The dopamine D3 receptor: a therapeutic target for the treatment of neuropsychiatric disorders. CNS Neurol Disord Drug Targets 5:25–43
4. Le Foll B, Diaz J, Sokoloff P (2005) Neuroadaptations to hyperdopaminergia in dopamine D3 receptor-deficient mice. Life Sci 76(11):1281–1296
5. Maina FK, Mathews TA (2010) A functional fast scan cyclic voltammetry assay to characterize dopamine D2 and D3 autoreceptors in the mouse striatum. ACS Chem Neurosci 1(6):450–462
6. Missale C, Nash SR, Robinson SW, Jaber M, Caron MG (1998) Dopamine receptors: from structure to function. Physiol Rev 78(1):189–225
7. Beaulieu JM, Gainetdinov RR (2011) The physiology, signaling, and pharmacology of dopamine receptors. Pharmacol Rev 63(1):182–217. doi:10.1124/pr.110.002642
8. Fiorentini C, Savoia P, Bono F, Tallarico P, Missale C (2015) The D3 dopamine receptor: from structural interactions to function. Eur Neuropsychopharmacol 25(9):1462–1469. doi:10.1016/j.euroneuro.2014.11.021
9. Todd RD (1992) Neural development is regulated by classical neurotransmitters: dopamine D2 receptor stimulation enhances neurite outgrowth. Biol Psychiatry 31(8):794–807
10. Spencer GE, Klumperman J, Syed NI (1998) Neurotransmitters and neurodevelopment. Role of dopamine in neurite outgrowth, target selection and specific synapse formation. Perspect Dev Neurobiol 5(4):451–467
11. Belinsky GS, Sirois CL, Rich MT, Short SM, Moore AR, Gilbert SE, Antic SD (2013) Dopamine receptors in human embryonic stem cell neurodifferentiation. Stem Cells Dev 22(10):1522–1540. doi:10.1089/scd.2012.0150
12. Van Kampen JM, Robertson HA (2005) A possible role for dopamine D3 receptor stimulation in the induction of neurogenesis in the adult rat substantia nigra. Neuroscience 136:381–386
13. O'Keeffe GC, Tyers P, Aarsland D, Dalley JW, Barker RA, Caldwell MA (2009) Dopamine-induced proliferation of adult neural precursor cells in the mammalian subventricular zone is mediated through EGF. Proc Natl Acad Sci U S A 106(21):8754–8759. doi:10.1073/pnas.0803955106
14. Kim Y, Wang WZ, Comte I, Pastrana E, Tran PB, Brown J, Miller RJ, Doetsch F et al (2010) Dopamine stimulation of postnatal murine subventricular zone neurogenesis via the D3 receptor. J Neurochem 114(3):750–760. doi:10.1111/j.1471-4159.2010.06799.x
15. Collo G, Bono F, Cavalleri L, Plebani L, Merlo Pich E, Millan MJ, Spano PF, Missale C (2012) Pre-synaptic dopamine D(3) receptor mediates cocaine-induced structural plasticity in mesencephalic dopaminergic neurons via ERK and Akt pathways. J Neurochem 120:765–778
16. Collo G, Zanetti S, Missale C, Spano PF (2008) Dopamine D3 receptor-preferring agonists increase dendrite arborization of mesencephalic dopaminergic neurons via extracellular signal-regulated kinase phosphorylation. Eur J Neurosci 28:1231–1240
17. Kim SY, Choi KC, Chang MS, Kim MH, Kim SY, Na YS, Lee JE, Jin BK et al (2006) The dopamine D2 receptor regulates the development of dopaminergic neurons via extracellular signal-regulated kinase and Nurr1 activation. J Neurosci 26(17):4567–4576
18. Yoon S, Choi MH, Chang MS, Baik JH (2011) Wnt5a-dopamine D2 receptor interactions regulate dopamine neuron development via extracellular signal-regulated kinase (ERK) activation. Biol Chem 286(18):15641–15651
19. Whone AL, Watt RL, Stoessl AJ, Davis M, Reske S, Nahmias C, Lang AE, Rascol O et al (2003) Slower progression of Parkinson's disease with ropinerole versus levodopa: the REAL-PET study. Ann Neurol 54:93–101
20. Van Kampen JM, Eckman CB (2006) Dopamine D3 receptor agonist delivery to a model of Parkinson's disease restores the nigrostriatal pathway and improves locomotor behavior. J Neurosci 26:7272–7280
21. Bellucci A, Collo G, Sarnico I, Battistin L, Missale C, Spano P (2008) Alpha-synuclein aggregation and cell death triggered by energy deprivation and dopamine overload are counteracted by D2/D3 receptor activation. J Neurochem 106(2):560–577. doi:10.1111/j.1471-4159.2008.05406.x
22. Benskey MJ, Perez RG, Manfredsson FP (2016) The contribution of alpha synuclein to neuronal survival and function - implications for Parkinson's disease. J Neurochem 37(3):331–359. doi:10.1111/jnc.13570
23. Takahashi K, Tanabe K, Ohnuki M, Narita M, Ichisaka T, Tomoda K, Yamanaka S (2007) Induction of pluripotent stem cells from adult human fibroblasts by defined factors. Cell 131:861–872
24. Yu J, Vodyanik MA, Smuga-Otto K, Antosiewicz-Bourget J, Frane JL, Tian S, Nie J, Jonsdottir GA et al (2007) Induced pluripotent stem cell lines derived from human somatic cells. Science 318(5858):1917–1920

25. Chambers SM, Fasano CA, Papapetrou EP, Tomishima M, Sadelain M, Studer L (2009) Highly efficient neural conversion of human ES and iPS cells by dual inhibition of SMAD signaling. Nat Biotechnol 27(3):275–280. doi:10.1038/nbt.1529
26. Kriks S, Shim JW, Piao J, Ganat YM, Wakeman DR, Xie Z, Carrillo-Reid L, Auyeung G et al (2011) Dopamine neurons derived from human ES cells efficiently engraft in animal models of Parkinson's disease. Nature 480(7378):547–551
27. Hartfield EM, Yamasaki-Mann M, Ribeiro Fernandes HJ, Vowles J, James WS, Cowley SA, Wade-Martins R (2014) Physiological characterisation of human iPS-derived dopaminergic neurons. PLoS One 9(2):e87388. doi:10.1371/journal.pone.0087388
28. Zaltieri M, Grigoletto J, Longhena F, Navarria L, Favero G, Castrezzati S, Colivicchi MA, Della Corte L et al (2015) α-synuclein and synapsin III cooperatively regulate synaptic function in dopamine neurons. J Cell Sci 128:2231–2243
29. Schmidt U, Beyer C, Oestreicher AB, Rejsert I, Schilling K, Pilgrim C (1996) Activation of dopaminergic D1 receptors promotes morphogenesis of developing striatal neurons. Neurosci 74:453–460
30. Maherali N, Ahfeldt T, Rigamonti A, Utikal J, Cowan C, Hochedlinger K (2008) A high-efficiency system for the generation and study of human induced pluripotent stem cells. Cell Stem Cell 3(3):340–345
31. Tucker RP (1990) The roles of microtubule-associated proteins in brain morphogenesis: a review. Brain Res Brain Res Rev 15(2):101–120
32. Picciotto MR, Zoli M, Rimondini R, Léna C, Marubio LM, Pich EM, Fuxe K, Changeux JP (1998) Acetylcholine receptors containing the beta2 subunit are involved in the reinforcing properties of nicotine. Nature 391:173–177
33. Changeux JP (2010) Nicotine addiction and nicotinic receptors: lessons from genetically modified mice. Nat Rev Neurosci 11:389–401
34. Chen P-C, Lao C-L, Chen J-C (2009) The D3 dopamine receptor inhibits dopamine release in PC-12/hD3 cells by autoreceptor signaling via PP-2B, CK1, and Cdk-5. J Neurochem 110(4):1180–1190. doi:10.1111/j.1471-4159.2009.06209
35. Collo G, Bono F, Cavalleri L, Plebani L, Mitola S, Merlo Pich E, Millan MJ, Zoli M et al (2013) Nicotine-induced structural plasticity in mesencephalic dopaminergic neurons is mediated by dopamine D3 receptors and Akt-mTORC1 signaling. Mol Pharmacol 83(6):1176–1189
36. Reith ME, Coffey LL, Xu C, Chen N-H (1994) GBR 12909 and 12935 block dopamine uptake into brain synaptic vesicles as well as nerve endings. Eur J Pharmacol 253(1–2):175–178
37. Swarzenski BC, Tang L, Oh YJ, O'Malley KL, Todd RD (1994) Morphogenic potentials of D2, D3, and D4 dopamine receptors revealed in transfected neuronal cell lines. Proc Natl Acad Sci U S A 91(2):649–653
38. Höglinger GU, Rizk P, Muriel MP, Duyckaerts C, Oertel WH, Caille I, Hirsch EC (2004) Dopamine depletion impairs precursor cell proliferation in Parkinson disease. Nat Neurosci 7(7):726–735
39. Baker SA, Baker KA, Hagg T (2004) Dopaminergic nigrostriatal projections regulate neural precursor proliferation in the adult mouse subventricular zone. Eur J Neurosci 20(2):575–579
40. Reinhardt P, Schmid B, Burbulla LF, Schöndorf DC, Wagner L, Glatza M, Höing S, Hargus G et al (2013) Genetic correction of a LRRK2 mutation in human iPSCs links parkinsonian neurodegeneration to ERK-dependent changes in gene expression. Cell Stem Cell 12(3):354–367. doi:10.1016/j.stem.2013.01.008
41. Alonso M, Medina JH, Pozzo-Miller L (2004) ERK1/2 activation is necessary for BDNF to increase dendritic spine density in hippocampal CA1 pyramidal neurons. Learn Mem 11:172–178
42. Kumar V, Zhang M-X, Swank MW, Kunz J, Wu G-Y (2005) Regulation of dendritic morphogenesis by Ras-PI3K-Akt-mTOR and Ras-MAPK signaling pathways. J Neurosci 25:11288–11299
43. Thomas GM, Huganir RL (2004) MAPK cascade signalling and synaptic plasticity. Nat Rev Neurosci 5:173–183
44. Rivera A, Trías S, Peñafiel A, Angel Narváez J, Díaz-Cabiale Z, Moratalla R, de la Calle A (2003) Expression of D4 dopamine receptors in striatonigral and striatopallidal neurons in the rat striatum. Brain Res 989:35–41
45. Rondou P, Haegeman G, Van Craenenbroeck K (2010) The dopamine D4 receptor: biochemical and signalling properties. Cell Mol Life Sci 67:1971–1986
46. Khan ZU, Gutiérrez A, Martín R, Peñafiel A, Rivera A, De La Calle A (1998) Differential regional and cellular distribution of dopamine D2-like receptors: an immunocytochemical study of subtype-specific antibodies in rat and human brain. J Comp Neurol 402:353–371
47. Fiorentini C, Gardoni F, Spano P, Di Luca M, Missale C (2003) Regulation of dopamine D1 receptor trafficking and desensitization by oligomerization with glutamate N-methyl-D-aspartate receptors. J Biol Chem 278:20196–20202
48. Liu F, Wan Q, Pristupa ZB, Yu XM, Wang YT, Niznik HB (2000) Direct protein-protein coupling enables cross-talk between dopamine D5 and gamma-aminobutyric acid a receptors. Nature 403:274–280
49. Quarta D, Ciruela F, Patkar K, Borycz J, Solinas M, Lluis C, Franco R, Wise RA et al (2007) Heteromeric nicotinic acetylcholine-dopamine autoreceptor complexes modulate striatal dopamine release. Neuropsychopharmacology 32:35–42
50. Lüscher C, Malenka RC (2011) Drug-evoked synaptic plasticity in addiction: from molecular changes to circuit remodeling. Neuron 69(4):650–663. doi:10.1016/j.neuron.2011.01.017
51. Olive MF, Gass JT (2015) Editorial: structural plasticity induced by drugs of abuse. Front Pharmacol 6:88. doi:10.3389/fphar.2015.00088
52. Benowitz NL (2010) Nicotine addiction. N Engl J Med 362(24):2295–2303. doi:10.1056/NEJMra0809890
53. Weiss HD, Marsh L (2012) Impulse control disorders and compulsive behaviors associated with dopaminergic therapies in Parkinson disease. Neurol Clin Pract 2(4):267–274
54. Holden C (2001) 'Behavioral' addictions: do they exist? Science 294(5544):980–982
55. Xilouri M, Brekk OR, Stefanis L (2013) α-synuclein and protein degradation systems: a reciprocal relationship. Mol Neurobiol 47(2):537–551. doi:10.1007/s12035-012-8341-2
56. Shannon KM, Bennett JP Jr, Friedman JH (1997) Efficacy of pramipexole, a novel dopamine agonist, as monotherapy in mild to moderate Parkinson's disease. The pramipexole study group. Neurology 49(3):724–728
57. Li C, Biswas S, Li X, Dutta AK, Le W (2010) Novel D3 dopamine receptor-preferring agonist D-264: evidence of neuroprotective property in Parkinson's disease animal models induced by 1-methyl-4-phenyl-1,2,3,6-tetrahydropyridine and lactacystin. J Neurosci Res 88(11):2513–2523. doi:10.1002/jnr.22405
58. Barreto GE, Iarkov A, Moran VE (2015) Beneficial effects of nicotine, cotinine and its metabolites as potential agents for Parkinson's disease. Front Aging Neurosci 6:340. doi:10.3389/fnagi.2014.00340
59. Ono K, Hirohata M, Yamada M (2007) Anti-fibrillogenic and fibril-destabilizing activity of nicotine in vitro: implications for the prevention and therapeutics of Lewy body diseases. Exp Neurol 205(2):414–424
60. Hong DP, Fink AL, Uversky VN (2009) Smoking and Parkinson's disease: does nicotine affect alpha-synuclein fibrillation? Biochim Biophys Acta 1794(2):282–290. doi:10.1016/j.bbapap.2008.09.026
61. Kalia LV, Lang AE (2015) Parkinson's disease. Lancet 386(9996):896–912. doi:10.1016/S0140-6736(14)61393-3
62. Caughey B, Lansbury PT (2003) Protofibrils, pores, fibrils, and neurodegeneration: separating the responsible protein aggregates from the innocent bystanders. Annu Rev Neurosci 26:267–298
63. Uversky VN, Eliezer D (2009) Biophysics of Parkinson's disease: structure and aggregation of alpha-synuclein. Curr Protein Pept Sci 10(5):483–499